of its features have been investigated through electromagnetic and circuit theory analyses and theoretical discussions have been checked by simulations. The structure can provide both reflective and transfer characteristics of a cavity, for both filter and oscillator applications. A three-pole filter has been designed and manufactured using this coupling structure, as one of the possible filter applications. The filter has an acceptable response in spite of its low degree, easy design, and fabrication process. In fact, the steepness of the filter in both cut-off frequencies has benefited from the zeros in transfer response of the cavities. The zeros can also be used for oscillator design which needs cavities to reflect energy in some frequencies and can be considered for further analysis.

REFERENCES

1. K. Wu, D. Deslandes, and Y. Cassivi, The substrate integrated circuits—A new concept for high-frequency electromagnetic and optoelectronics, Mikrotalasna revija, (2003), 2–9.
2. A. Borji, D. Busuioc, and S. Safavi-Naeini, Efficient, low-cost integrated waveguide-fed planar antenna array for Ku-band applications, Antennas Wireless Propag Lett 8 (2009), 336–339.
3. K. Saeed, R.D. Pollard, and I.C. Hunter, Substrate integrated waveguide cavity resonators for complex permittivity characterization of materials, IEEE Trans Microwave Theory Tech 56 (2008), 2340–2347.
4. Y. Cassivi and K. Wu, Low cost microwave oscillator using substrate integrated waveguide cavity, IEEE Microwave Wireless Components Lett 13 (2003), 48–50.
5. Y.L. Zhang, W. Hong, K. Wu, J. X. Chen, and H.J. Tang, Novel substrate integrated waveguide cavity filter with defected ground structure, IEEE Trans Microwave Theory Tech 53 (2005), 1280–1287.
6. Y. Cassivi, L. Perregrini, K. Wu and G. Conciauro, Low-cost and high-Q millimeter-wave resonator using substrate integrated waveguide technique, In: European Microwave Conference, 2002, Vol. 2. September 2002, Milan.
7. A. El-Tager, J. Bray, and L. Roy, High-Q LTCC Resonators for millimeter wave applications, In: Microwave Symposium Digest (IEEE MTT-S), Philadelphia, PA, Vol. 3, 2003, pp. 2257–2260.
8. Q.F. Wei, Z.F. Li, L. Li, W.J. Zhang, and J.F. Mao, Three-pole cross-coupled substrate-integrated waveguide bandpass filters based on PCB process and multilayer LTCC technology, Microwave Opt Tech Lett 51 (2009), 71–73.
9. A. Ismail, M.S. Razalli, M.A. Mahdi, R.S.A.R. Abdullah, N.K. Noordin, and M.F.A. Rasid, X-Band trisection substrate-integrated waveguide quasi-elliptic filter, Prog Electromagn Res 85 (2008), 133–145.
10. A. Suntives and R. Abhari, Transition structures for 3-D integration of substrate integrated waveguide interconnects, IEEE Microwave Wireless Components Lett 17 (2007), 697–699.
11. C. Yau, T.Y. Huang, T.M. Shen, H.Y. Chien, and R.B. Wu, Design of 30 GHz Transition between microstrip line and substrate integrated waveguide, In: Proceedings of Asia-Pacific Microwave Conference, Bangkok, Thailand, 2007.
12. Y. Ding, and K. Wu, Substrate integrated waveguide-to-microstrip transition in multilayer substrate, IEEE Trans Microwave Theory Tech 55 (2007).
13. I.W. Lee, S.H. Han, T.S. Yun, H. Nam, S.Y. Oh, and J.C. Lee, A new substrate integrated waveguide (SIW) cavity resonator with reflective characteristic, In: Proceedings of Asia-Pacific Microwave Conference, Bangkok, Thailand, 2007.
14. J.C. Bohorquez, B. Potelon, C. Person, E. Rius, C. Quendo, G. Tanne, and E. Fourn, Reconfigurable planar SIW cavity resonator and filter, In: Microwave Symposium Digest, San Francisco, CA, June 2006, IEEE MTT-S, pp. 947–950.
15. Y. Cassivi, L. Perregrini, P. Arcioni, M. Bressan, K. Wu, and G. Conciauro, Dispersion characteristics of substrate integrated rectangular waveguide, IEEE Microwave Wireless Components Lett 12 (2002), 333–335.
16. F. Xu and K. Wu, Guided-wave and leakage characteristics of substrate integrated waveguide, IEEE Trans Microwave Theory Tech 53 (2005), 6–73.
17. W. Che, K. Deng, D. Wang, and Y.L. Chow, Analytical equivalence between substrate-integrated waveguide and rectangular waveguide, IET Microwave Antennas Propag 2 (2008), 35–41.
18. R.F. Harrington, Time-harmonic electromagnetic fields, IEEE, 2001, New York, NY, pp. 227–228 and 317–319.
19. J.S. Hong, and M.J. Lancaster, Microstrip filters for RF/microwave applications, John Wiley & Sons Inc., New York, NY, 2001, pp. 151–155.

DEMONSTRATION OF ACOUSTIC VIBRATION SENSOR BASED ON MICROFIBER KNOT RESONATOR

A. Sulaiman,[1] M. Z. Muhammad,[1] S. W. Harun,[1,2] H. Arof,[1] and H. Ahmad[2]
[1] Faculty of Engineering, Department of Electrical Engineering, University of Malaya, 50603 Kuala Lumpur, Malaysia; Corresponding author: swharun@um.edu.my
[2] Photonics Research Centre, University of Malaya 50603, Kuala Lumpur, Malaysia

Received 15 September 2012

ABSTRACT: *A compact microfiber-based acoustic vibration sensor is demonstrated using microfiber knot resonator (MKR) structure, which is fabricated by flame brushing technique. It is observed that the extinction ratio of the resonant spectrum of the knot resonator is linearly proportional to the vibration amplitude. This is attributed to the interruption of the effective coupling of the MKR which is correlated with the exposed vibration force. It is also shown that the resonant wavelength shifts by about 0.19 nm as the normalized vibration energy is increased from 0 to 10%. The performance of the sensor is then further investigated by monitoring the fast Fourier transform (FFT) of the signal when the MKR is exposed to various vibration frequencies as a narrowband 1545 nm laser is injected into the MKR. In the spectra of the signals, the frequency of the applied vibration is clearly shown as it has the highest magnitude followed by the accompanying harmonics. This holds true for all vibration frequencies.* © 2013 Wiley Periodicals, Inc. Microwave Opt Technol Lett 55:1138–1141, 2013; View this article online at wileyonlinelibrary.com. DOI 10.1002/mop.27526

Key words: *acoustic sensors; microfiber; knot resonator; vibration sensors*

1. INTRODUCTION

In recent years, interest in vibration sensors has grown as they are found to be useful for monitoring the condition of rotating machinery, where excessive vibration could indicate overloading, inadequate lubrication, or bearing wear [1–5]. Commercial vibration sensors use a piezoelectric ceramic strain transducer attached to a metallic proof mass in order to respond to an externally imposed acceleration. This technique is very popular but it requires the probe to be in contact with the moving object. Many optical methods have been proposed in the literatures since they provide excellent technologies to develop non-contact sensors [2, 3]. In interferometric method, a laser signal beam is directed onto a moving target and the back-reflected light is recombined with part of the incident light, using techniques such as Michelson or Mach–Zendher schemes [4]. Interferometers are high in performance but also very expensive. They also impose stringent mechanical requirements as the alignment is critical. Laser vibrometer exploits Doppler effect [5] to measure the amplitude of the vibration. This sensor is quite expensive

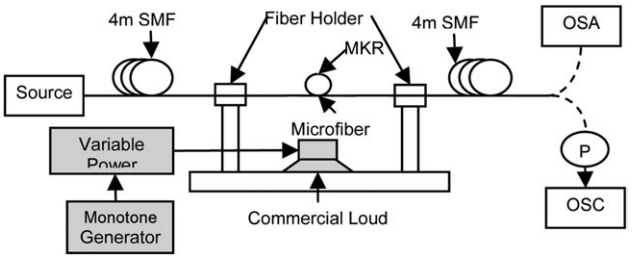

Figure 1 The schematic diagram of the experimental setup. The microfiber is fabricated through flame brush technique. The MKR loop diameter is 3 mm

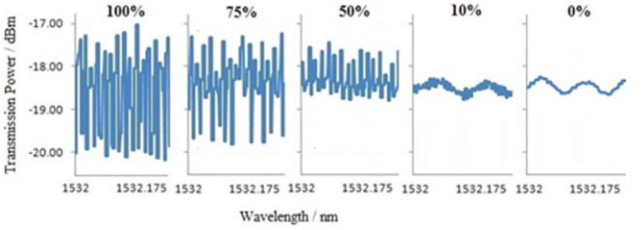

Figure 3 Resonant spectrum of the MKR at various normalized vibration energy. [Color figure can be viewed in the online issue, which is available at wileyonlinelibrary.com]

and not accurate enough for precise measurement of minute displacements.

Of late, there is growing interest on fiber optic sensors as they offer many advantages compared to conventional electrical ones such as being light weight, compact, non-contact, electrically isolated, immune to electromagnetic interference, and perturbation-free. In addition, fiber sensors are an attractive solution due to the possibility of integrating a large number of sensors by multiplexing and interrogation techniques in photonic domain. Recently, efforts have been expended to develop microfiber knot resonators (MKRs) that can serve as optical filters for many potential applications in optical communication and sensors [6–9]. They can be assembled by inter-twisting and coupling two microfibers to form a resonator via micro-manipulation. In comparison with a microfiber loop resonator (MLR), an MKR does not rely solely on van der Waals attraction force to maintain the coupling region since the two fibers are twisted to form a stronger coupling. In consequence, an MKR is more rigid and can better maintain its structure, thus producing a more stable resonance condition. In this article, a new application of the MKR is demonstrated for vibration sensor. The sensor can detect the vibration frequency of up to 800 Hz and the extinction ratio of the resonant spectrum of the knot resonator is observed to be linearly proportional to the vibration amplitude. To our knowledge this is the first demonstration of an MKR-based acoustic vibration sensor.

2. EXPERIMENT

The schematic representation of the experimental setup for the MKR-based vibration sensor is shown in Figure 1. The sensor consists of an amplified spontaneous emission (ASE) source, MKR probe, load speaker, audio amplifier, monotone generator and an optical spectrum analyzer. The MKR was fabricated using a standard single mode fiber (SMF). A small section of the SMF (about 3 cm long) is stripped and pulled tautly by two fiber holders on the fabrication stage. A fine thin and low loss microfiber is fabricated by heating and stretching of the stripped SMF until the waist diameter reduces to about 1 μm via flame brushing technique. The fabricated microfiber is then cut into 2 unequal parts to assemble the MKR by micro-manipulation. The longer part of the microfiber is twisted to form a large loop and the end of the microfiber is inserted inside the loop to form a knot. The required loop diameter is obtained by gradually pulling one of the fiber ends. The shorter part of the microfiber is coupled to the knot by van der Waals force to collect the light transmitted out of the knot by means of evanescent coupling. The knot configuration is maintained by elastic-bend-induced tensile force and friction at the intertwisted area and thus ensures the structural stability of the device.

In the experiment, a commercial high power speaker is placed closely under the fabricated MKR structure, which is located in between the fiber holders. These fiber holders and speaker are fixed on the same base metal plate as shown in Figure 1. The monotone generator is capable of generating a signal with a frequency varying from 1 to 3 MHz. The signal is amplified by the power amplifier before it is injected into the speaker. The speaker transforms the monotone frequency from the generator into acoustic energy (vibration), which then vibrates the MKR structure. The output signal from the MKR is analyzed by an Optical Society of America (OSA) at various amplitudes of the injected acoustic signal. The experiment is then repeated by replacing the ASE source with a signal wavelength laser operating at 1545 nm while the output signal is detected by a photodetector and analyzed by an oscilloscope.

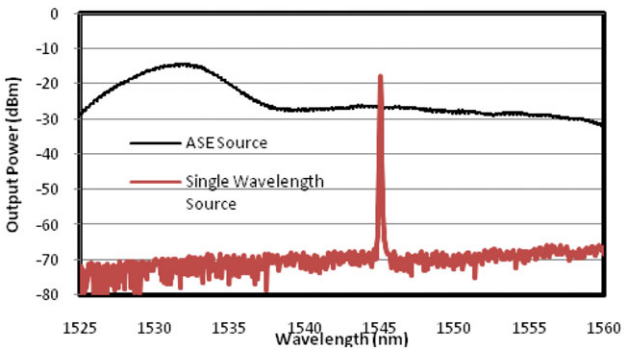

Figure 2 Output Spectra from both light sources used in this experiment. [Color figure can be viewed in the online issue, which is available at wileyonlinelibrary.com]

3. RESULTS AND DISCUSSION

Figure 2 shows the spectrum characteristic of both light sources used in this experiment. The broadband ASE operates within a wavelength region from 1510 to 1560 nm with the maximum power of around −17 dBm. The single-wavelength laser operates at 1545 nm with peak power of −18 dBm. In the first experiment, the ASE light is launched into the MKR while a constant acoustic sinusoidal wave operating at 100 Hz is applied to the structure. The acoustic wave power is generated by a monotone generator where the vibration intensity can be varied by a variable power amplifier. Figure 3 shows the resonant spectrum of the MKR at various normalized vibration energy from idle case (0%) up to 100% vibration energy. As seen, the extinction ratio of the spectrum increases as the vibration energy increases. This is attributed to the vibration energy which modulates the intensity coupling ratio of the MKR and increases the extinction ratio of the output spectrum. It is also observed that

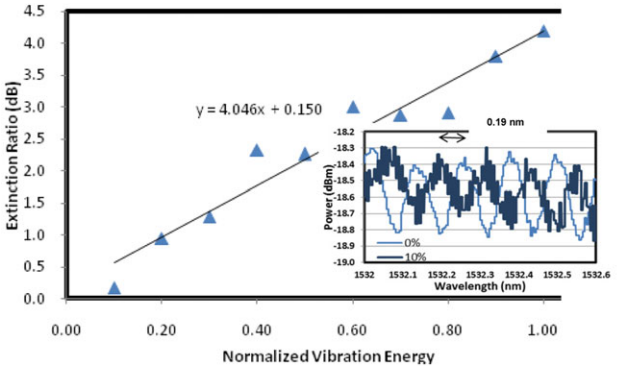

Figure 4 Extinction ratio against normalized vibration energy. Inset compares the resonant spectrum with and without vibration energy. [Color figure can be viewed in the online issue, which is available at wileyonlinelibrary.com]

the resonant is back to original resonant spectrum in term of position and shape when the vibration energy is cut off.

The transmission of the MKR is given by the following Eq. (1):

$$T = \frac{e^{-\alpha L/2}e^{j\beta L} - \sin \kappa l}{1 - e^{-\alpha L/2}e^{j\beta L} \sin \kappa l} \tag{1}$$

where α is the intensity attenuation constant, β is the propagation constant along the microfiber, L represents the round trip length of the resonator, and $\sin(K)$ represents the intensity coupling ratio. K is directly related to the coupling length and it can be expressed as

$$K = \kappa l \tag{2}$$

where κ is the coupling coefficient and l is the coupling length. The vibration energy modulates the coupling ratio of the MKR and consequently varies the transmission characteristic of the MKR. This increases of the extinction ratio of the output spectrum of the MKR. Figure 4 shows the extinction ratio as a function of the normalized vibration energy. The average extinction ratio is seen to be directly proportional to the vibration energy. The resonant spectrum is also shifted with the vibration as shown in the inset of Figure 4. It is shown that the resonant wavelength shifts by about 0.19 nm as the normalized vibration energy is increased from 0 to 10%. This is most probably due to the acoustic vibration, which might change the refractive index of the MKR due to the applied strain. The change in the refractive index varies the phase of the propagating light inside the MKR, which in turn shifts the resonant wavelength.

The performance of the MKR-based vibration sensor is also investigated using a narrow band laser source while the output

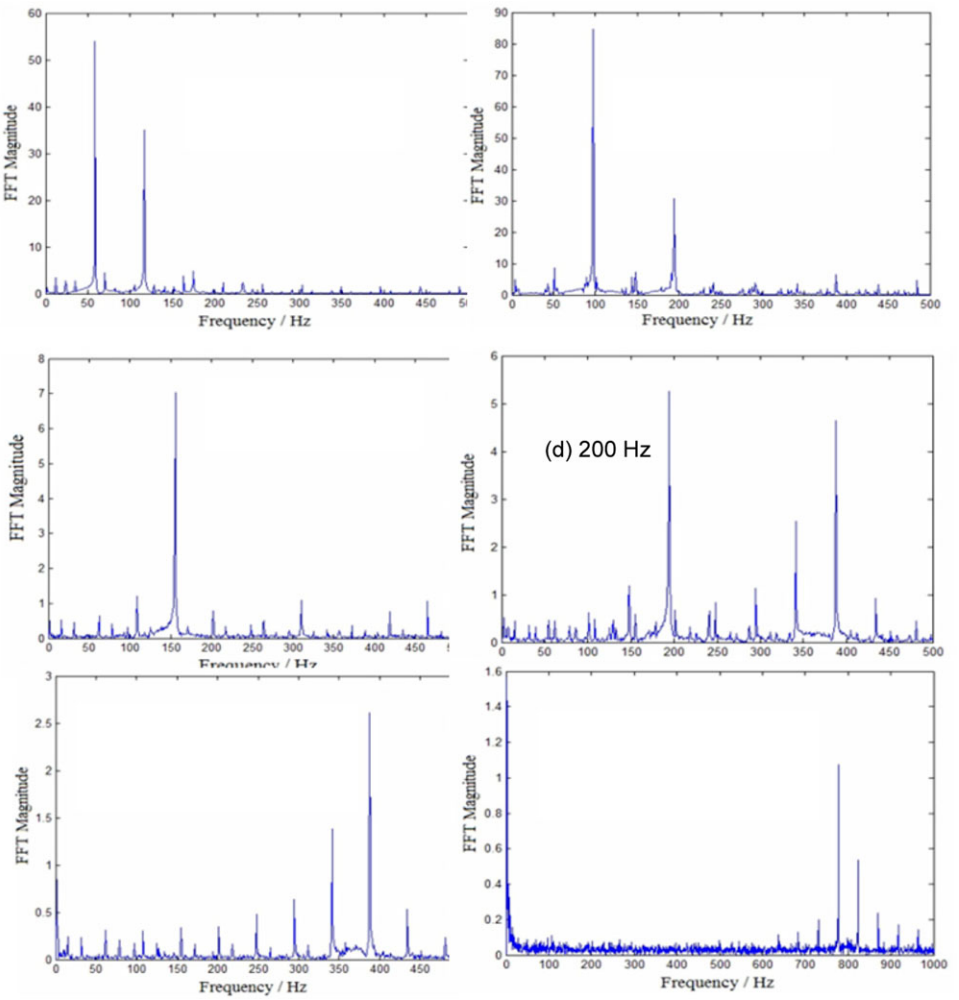

Figure 5 FFT spectral responses at various vibration frequencies (a) 60 Hz, (b) 100 Hz, (c) 160 Hz, (d) 200 Hz, (e) 400 Hz, and (f) 800 Hz. [Color figure can be viewed in the online issue, which is available at wileyonlinelibrary.com]

signal is detected by a photo-detector and analyzed by an oscilloscope. The ASE source is then replaced by a signal wavelength laser operating at 1545 nm and the vibration frequency is varied from 60 Hz to 800 Hz. Figure 5 shows the extracted fast Fourier transform (FFT) signal from the oscilloscope at various vibration frequencies. From the figure, the FFT signal shows that the applied vibration wave frequency has the highest magnitude followed by the accompanying harmonic for all spectra. This is attributed to the compression and rarefaction of the imparted acoustic waves, which cause the optical phase to change. This shows that the modulation of the vibration acoustic wave can be translated into the modulation of the output signal frequency. One of the main challenges of understanding the proposed sensor is the find out the correct mechanism to impart the vibration energy to the MKR. The adopted setup consisting of a metal base with fiber holders and a non-mobile speaker only allows the sensing of vibration frequency up to 1 KHz. For frequency higher than 1 KHz, the setup becomes less responsive to the input, as the magnitude of the FFT spectra of the output diminishes. This is probably due to the effect of excessive vibration on the structure of the MKR. Thus, a better solution is necessary when transferring energy of higher frequency vibration to the MKR without disrupting its structure especially at the coupling area.

4. CONCLUSION

A compact simple and low-cost acoustic vibration sensor is demonstrated using an MKR structure as a probe for the first time. The MKR is fabricated by knotting a microfiber, which is obtained by heating and stretching an SMF via flame brushing technique. The sensor can detect the vibration frequency up to 800 Hz while the extinction ratio of the resonant spectrum of the knot resonator is observed to be linearly proportional to the vibration amplitude. This is attributed to the interruption of the effective coupling of the MKR which is in correlation with the exposed vibration force. It is also observed that the resonant wavelength shifts by about 0.19 nm as the normalized vibration energy is changed from 0 to 10%. The frequency of the launched acoustic vibration wave can be retrieved back using FFT technique. The extracted FFT signals clearly show that the applied vibration wave frequency has the highest magnitude followed by the accompanying harmonics.

ACKNOWLEDGMENTS

S. W. Harun acknowledges a financial support by University of Malaya Research Grant Scheme (Grant No: RG144-12AET).

REFERENCES

1. P.M.B.S. Girao, O.A. Postolache, J. Faria, and J.M.C.D. Pereira, An overview and a contribution to the optical measurement of linear displacement, IEEE Sensors J 1 (2001), 322–331.
2. T.K. Gangopadhyay, Prospects for fibre Bragg gratings and Fabry-Perot interferometers in fibre-optic vibration sensing, Sensors Actuators A 113 (2004), 20–38.
3. G. Perrone and A. Vallan, A low-cost optical sensor for noncontact vibration measurements, IEEE Trans Instrum Meas 58 (2009), 1650–1656.
4. G. Song, X. Wang, and Z. Fang, White-light interferometer with high sensitivity and resolution using multi-mode fibers, Optik 112 (2011), 245–249.
5. P. Castellini, M. Martarelli, and E.P. Tomasini, Laser Doppler Vibrometry: Development of advanced solutions answering to technology's needs, Mech Syst Signal Process 20 (2006), 1265–1285.
6. K.S. Lim, A.A. Jasim, S.S.A. Damanhuri, S.W. Harun, B.M.A. Rahman, and H. Ahmad, Resonance condition of a microfiber knot resonator immersed in liquids, Appl Opt 50 (2011), 5912–5916
7. A. Sulaiman, S.W. Harun, F. Ahmad, S.F. Norizan, and H. Ahmad, Electrically tunable microfiber knot resonator based erbium-doped fiber laser, IEEE J Quantum Electron 48 (2012), 443–446.
8. A. Sulaiman, S.W. Harun, K.S. Lim, F. Ahmad, and H. Ahmad, Tunable laser generation with erbium-doped microfiber knot resonator, Laser Phys 22 (2012), 1–4.
9. K.S. Lim, S.W. Harun, S.S.A. Damanhuri, A.A. Jasim, C.K. Tio, and H. Ahmad, ''Current sensor based on microfiber knot resonator'' Sensors and Actuators A, vol. 167, pp. 60–62 (2011).

A RECONFIGURABLE ANTENNA USING VARACTOR DIODE FOR LTE MIMO APPLICATIONS

Cheol Yoon,[1] Sun-Gook Hwang,[1] Gi-Chan Lee,[1] Woo-Su kim,[2] Hwa-Choon Lee,[3] and Hyo-Dal Park[1]

[1] Department of Electronic Engineering, Inha University, 253 YongHyun-dong, Nam-gu, Incheon 402-751, Republic of Korea; Corresponding author: drunken2@nate.com

[2] Information and Communication Engineering, KEIT, 701-7 Yeoksam-dong, Gangnam-gu, Seoul 135-080, Republic of Korea

[3] Department of Information and Communications Engineering, Chodang University, 429 SungNam-li, Muan-eup, Muan-gun, Cheon-nam 534-800, Republic of Korea

Received 15 August 2012

ABSTRACT: *In this article, a mobile embedded antenna having tunable capacitance is proposed and the validity of the proposed solution was proved through design, fabrication, and measurement. The antenna can be applied to long-term evolution (LTE) as well as DCS/PCS/WCDMA bands being currently used. Antennas for the 4G mobile service are required to expand its bandwidth so that it includes both LTE band and other service bands. However, it is hard to obtain low-band characteristic due to the limited space for antenna in terminals. The proposed antenna consists of two planar inverted F antennas that are orthogonally arranged. Two radiators should be designed to have equal or enhanced isolation (S_{21}) of lower than −15 dB. To meet this requirement, a varactor diode SMV2109 (skyworks corp.) was used to make the operation frequency of low-band tunable. With the optimized parameters, the antenna was fabricated and measured and the results have been compared with the simulated result. The antenna satisfied with operation frequency and performance for both low-band and high-band, and measured performance of the antenna fabricated with optimized parameters is compared and analyzed with the simulation results.* © 2013 Wiley Periodicals, Inc. Microwave Opt Technol Lett 55:1141–1145, 2013; View this article online at wileyonlinelibrary.com. DOI 10.1002/mop.27479

Key words: *reconfigurable antenna; varactor diode; long-term evolution; multiple-input multiple-output*

1. INTRODUCTION

Recently, as there has been huge improvement in mobile communication technology, communication systems are being diversified. Researches on the communication systems such as long-term evolution (LTE), ultra mobile broadband, and Mobile Wimax (Wibro + CDMA) have been carried out, and LTE was adopted as a 4G communication system in most countries [1, 2]. The LTE mobile communication system provides high speed transfer about 100 Mbps of downlink and 50 Mbps of uplink in low speed move, and 30 Mbps of downlink and 15 Mbps of